Composite Structures
December 2002; 58(4) : 529-537
http://dx.doi.org/10.1016/S0263-8223(02)00162-9

Optimal laminations of thin underwater composite cylindrical vessels

Tanguy Messager[a*], Mariusz Pyrz[b], Bernard Gineste[c] and Pierre Chauchot[d]

[a]Laboratoire de Mécanique et Matériaux, UPRES EA 2166, Ecole Centrale de Nantes, BP 92101, 44321, Nantes cédex 3, France
[b]Laboratoire de Mécanique de Lille, URA CNRS 1441, Boulevard Paul Langevin, 59655, Villeneuve d'Ascq cédex, France
[c]Laboratoire de Rhéologie et de Mécanique des Structures, EA 940, Université de Bretagne Occidentale, 6 Avenue Le Gorgeu, BP 809, 29285, Brest cédex, France
[d]IFREMER, Service Matériaux et Structures, BP 70, 29280, Plouzané, France

*: Corresponding author : Tel.: +33-240-372-585; fax: +33-240-372-573; tanguy.messager@iut-nantes.univ-nantes.fr

Abstract: This paper deals with the optimal design of deep submarine exploration housings and autonomous underwater vehicles. The structures under investigation are thin-walled laminated composite unstiffened vessels. Structural buckling failure due to the high external hydrostatic pressure is the dominant risk factor at exploitation conditions. The search of fiber orientations of the composite cylinders that maximize the stability limits is investigated. A genetic algorithm procedure coupled with an analytical model of shell buckling has been developed to determine numerically optimized stacking sequences. Characteristic lamination patterns have been obtained. FEM analyses have confirmed the corresponding significant increases of buckling pressures with respect to initial design solutions. Experiments on thin glass/epoxy and carbon/epoxy cylinders have been performed. The measured buckling pressures appear to be in good agreement with numerical results and demonstrate the gains due to the optimized laminations.

Keywords: Composite; Cylinder; Lamination; Buckling; Optimal design; Experimental results

OPTIMAL LAMINATIONS OF THIN UNDERWATER COMPOSITE CYLINDRICAL VESSELS

Tanguy MESSAGER [*] ; Mariusz PYRZ [**] ; Bernard GINESTE [***] ; Pierre CHAUCHOT [****]

[*] *Laboratoire de Mécanique et Matériaux, UPRES EA 2166*
Ecole Centrale de Nantes, BP92101, 44321 Nantes cédex3, France
tanguy.messager@iut-nantes.univ-nantes.fr

[**] *Laboratoire de Mécanique de Lille, URA CNRS 1441*
Boulevard Paul Langevin, 59655 Villeneuve d'Ascq cédex, France
mariusz.pyrz@eudil.fr

[***] *Laboratoire de Rhéologie et de Mécanique des Structures, EA 940*
Université de Bretagne Occidentale
6 avenue Le Gorgeu, BP809, 29285 Brest cédex, France
bernard.gineste@univ-brest.fr

[****] *IFREMER, Service Matériaux et Structures*
BP70, 29280 Plouzané, France
pierre.chauchot@ifremer.fr

Abstract

This paper deals with the optimal design of deep submarine exploration housings and autonomous underwater vehicles. The structures under investigation are thin-walled laminated composite unstiffened vessels. Structural buckling failure due to the high external hydrostatic pressure is the dominant risk factor at exploitation conditions. The search of fiber orientations of the composite cylinders that maximize the stability limits is investigated. A genetic algorithm procedure coupled with an analytical model of shell buckling has been developed to determine numerically optimized stacking sequences. Characteristic lamination patterns have been obtained. FEM analyses have confirmed the corresponding significant increases of buckling pressures with respect to initial design solutions. Experiments of thin glass/epoxy and carbon/epoxy cylinders have been

performed. The measured buckling pressures appear to be in good agreement with numerical results and demonstrate the gains due to the optimized laminations.

Key-words

composite ; cylinder ; lamination ; buckling ; optimization ; experiments

1. Introduction

The use of composite materials for submersible structures, allowing low weight to displacement ratios and long endurance for devices of limited energy carrying capability, have been investigated in recent studies [1,2,3]. Various applications, such as submarine exploration housings and autonomous underwater vehicles, are currently developed by IFREMER (the French Research Institute for the Exploitation of the Sea) with participation in European BRITE and MAST programs [3,4]. Such deep-submersible vessels are unstiffened, lengthy , laminated, cross-ply cylinders having rigid metallic end-closures as shown in Fig. 1. These composite tubes are carbon reinforced or glass reinforced epoxy resin structures obtained by the filament winding process [5,6]. Most of the thin cylinders investigated so far in IFREMER's studies are based on $\lfloor \pm 55° \rfloor_N$ orthotropic sequences. This choice is classical for thin tubes subjected to internal pressure: due to the ratio between the circumferential and the axial load components resulting from the loading, the $\lfloor \pm 55° \rfloor_N$ laminations maximize the static strength [3,6].

The composite cylindrical vessels for underwater applications are intended to operate at high external hydrostatic pressure (sometimes up to 60 Mpa) [3]. Previous numerical and experimental studies performed by IFREMER have shown that failure due to structural buckling is the major risk factor for thin laminated cylinders [1,2,3]. The calculated and experimental buckling modes of the lengthy vessels are characterized by one longitudinal

half-wave and two (mode called ‘type 2’) or three (‘type 3’) circumferential half-waves as shown in Fig. 2. As noted in previous papers, the optimization of ply angles in order to maximize the buckling loads could take advantage of the potential of fiber-reinforced materials allowing the properties of the laminate to be tailored to the application [7,8,9]. Thus, the aim of this study is the improvement of lamination patterns increasing the stability limit of the composite laminated cylinders subjected to hydrostatic external pressure.

First, a numerical study has been carried out. An analytical buckling model of laminated cylinder has been coupled to a genetic algorithm procedure. This optimization tool allows the search for stacking sequences that maximize the buckling pressure and takes into account the manufacturing constraints. For all structures studied, a characteristic optimized lamination pattern has been obtained. Afterwards, the corresponding increases of buckling pressures calculated with respect to the $[\pm 55°_N]$ reference cylinders have been evaluated by FEM analyses. Next, the experimental investigation of a carbon/epoxy optimized cylinder has been achieved. Moreover, buckling tests of both optimized and $[\pm 55°_N]$ glass/epoxy thin cylinders have been performed on a specific experimental device in order to enable direct comparisons of experimental stability limits.

2. Numerical preliminary study of optimal lamination design

2.1. Formulation of the optimization problem

The geometry of a shell is characterized by its length *L*, its mean radius *R* and its wall-thickness *h* (see Fig. 3). The cylindrical wall is composed of *N* orthotropic plies of equal thickness. According to the filament winding manufacturing process, each ply is characterized by its filament-winding angle θ_i and is assumed to be cross-ply (i.e. made up

of equal amounts of fibers evenly distributed through its thickness in the $+\theta_i$ and $-\theta_i$ directions with respect to the cylinder axis). The stacking sequence is denoted by $[\theta_1 / \theta_2 / ... / \theta_N]$, where the angles are given in degrees, starting from the inner surface of the tube. The corresponding critical pressure is noticed P_{cr}. In addition, in a real-world manufacturing process, the filament-winding angles θ_i must be chosen from a limited set of M allowable values Θ_j according to technology references. Thus, the optimization problem becomes a discrete one comprising N^M potential lamination designs and can be expressed as follows:

find the best lamination: $\left[\theta_1 / \theta_2 / ... / \theta_N\right]_{OPTI}$
applying available angles: $\theta_i \in \{\Theta_1 ; \Theta_2 ; ... ; \Theta_M\}$
to maximize the buckling pressure: P_{cr}

2.2. Optimization tool

An optimization design tool has been created (computed in Fortran 90) to investigate numerically the optimized laminations increasing the buckling pressures of the filament wound cylinders. Its principle is described in Fig. 4. First, the initial parameters (geometry, number of plies and mechanical orthotropic properties of the constitutive composite material) are introduced. The search for the optimized lamination is performed by the coupling of analytical buckling shell models providing the buckling pressure value P_{cr} to a standard genetic algorithm optimization procedure. Finally, the optimization code gives the best lamination $[\theta_1 / \theta_2 / ... / \theta_N]_{OPTI}$ (corresponding to the highest P_{cr} calculated value) found by the optimization code.

2.2.1. Analytical buckling shell model

The analytical buckling model developed for laminated cylinders subjected to external pressure has been developed taking into consideration the following two assumptions:

- The instability phenomena is investigated for thin-walled laminated shells that are sensitive to transverse shear effects [4,6,10]. Thus, the approach developed is based on a Third Order Shear Deformable theory (TOSD) [11].
- In order to restrict the time of calculation to acceptable values for the developed optimization tool, the analytical model is based on the linear buckling theory. Such an approach may overestimate the buckling pressures [12] but it generally provides good sensitivity to lamination parameters, thus allowing the search for stacking sequences which increase the buckling pressure [9,12].

As shown in Fig. 3, the *x*, *y* and *z* coordinates and the corresponding *U*, *V* and *W* displacements are measured in the axial, circumferential and radial directions with respect to the cylindrical mean-surface [13]. The TOSD displacement field has been chosen so as to satisfy the transverse shear deformation conditions (i.e. ε_{xz} and ε_{yz} are zero on the shell external surfaces [11]). This field is expressed as follows:

$$\begin{cases} U = U(x,y,z) = u + z\varphi_x - z^3 \dfrac{4}{3h^2}\left(\dfrac{\partial w}{\partial x} + \varphi_x\right) \\ V = V(x,y,z) = v + z\varphi_y - z^3 \dfrac{4}{3h^2}\left(\dfrac{\partial w}{\partial y} + \varphi_y\right) \\ W = W(x,y,z) = w \end{cases} \quad (1)$$

Previous modeling studies [13,14] have shown that the composite cylinders considered can be assumed to be simply supported at their ends. The displacement approximation functions, satisfying these kinematic boundary conditions, are defined by [11,12]:

$$\begin{cases} u = u(x,y) = a_u \cdot \cos(\overline{m}x) \cdot \cos(\overline{n}y) \\ v = v(x,y) = a_v \cdot \sin(\overline{m}x) \cdot \sin(\overline{n}y) \\ w = w(x,y) = a_w \cdot \sin(\overline{m}x) \cdot \cos(\overline{n}y) \\ \varphi_x = \varphi_x(x,y) = a_{\varphi x} \cdot \cos(\overline{m}x) \cdot \cos(\overline{n}y) \\ \varphi_y = \varphi_y(x,y) = a_{\varphi y} \cdot \sin(\overline{m}x) \cdot \sin(\overline{n}y) \end{cases} \quad \text{with} \quad \begin{cases} \overline{m} = m\pi / L \\ \overline{n} = n / R \end{cases} \tag{2}$$

where m and n are numbers of longitudinal and circumferential half-waves of the buckling mode. The linear strain-displacement relations are [11]:

$$\begin{cases} \varepsilon_{xx} = \dfrac{\partial U}{\partial x} \\ \varepsilon_{yy} = \dfrac{1}{1+z/R}\left(\dfrac{\partial V}{\partial y} + \dfrac{W}{R}\right) \\ 2\varepsilon_{yz} = \dfrac{\partial V}{\partial z} + \dfrac{1}{1+z/R}\left(\dfrac{\partial W}{\partial y} - \dfrac{V}{R}\right) \\ 2\varepsilon_{xz} = \dfrac{\partial U}{\partial z} + \dfrac{\partial W}{\partial x} \\ 2\varepsilon_{xy} = \dfrac{\partial V}{\partial x} + \dfrac{1}{1+z/R}\dfrac{\partial U}{\partial y} \end{cases} \tag{3}$$

The elastic orthotropic constitutive law for the k^{th} composite cross-ply is given by [11]:

$$\begin{Bmatrix} \sigma_{xx} \\ \sigma_{yy} \\ \sigma_{yz} \\ \sigma_{xz} \\ \sigma_{xy} \end{Bmatrix} = \begin{bmatrix} C_{11}^{(k)} & C_{12}^{(k)} & 0 & 0 & 0 \\ & C_{22}^{(k)} & 0 & 0 & 0 \\ & & C_{44}^{(k)} & 0 & 0 \\ & & & C_{55}^{(k)} & 0 \\ +\text{sym.} & & & & C_{66}^{(k)} \end{bmatrix} \begin{Bmatrix} \varepsilon_{xx} \\ \varepsilon_{yy} \\ 2\varepsilon_{yz} \\ 2\varepsilon_{xz} \\ 2\varepsilon_{xy} \end{Bmatrix} \tag{4}$$

where the $C_{ij}^{(k)}$ terms are the corresponding orthotropic constitutive coefficients detailed in Ref. [6,12]. The force and moment resultants related to the mean-surface of the shell are

expressed as follows [12]:

$$\begin{Bmatrix} N_x \\ N_{xy} \\ T_x \\ M_x \\ M_{xy} \end{Bmatrix} = \int_{-h/2}^{h/2} \begin{Bmatrix} \sigma_{xx} \\ \sigma_{xy} \\ \sigma_{xz} \\ z\sigma_{xx} \\ z\sigma_{xy} \end{Bmatrix} \left(1 + \frac{z}{R}\right) \mathrm{d}z \qquad \text{and} \qquad \begin{Bmatrix} N_y \\ N_{yx} \\ T_y \\ M_y \\ M_{yx} \end{Bmatrix} = \int_{-h/2}^{h/2} \begin{Bmatrix} \sigma_{yy} \\ \sigma_{yx} \\ \sigma_{yz} \\ z\sigma_{yy} \\ z\sigma_{yx} \end{Bmatrix} \mathrm{d}z \tag{5}$$

The five governing equations of equilibrium are defined by [12]:

$$\begin{cases} \dfrac{\partial N_x}{\partial x} + \dfrac{\partial N_{yx}}{\partial y}_{x} = 0 \\ \dfrac{\partial N_y}{\partial y} + \dfrac{\partial N_{xy}}{\partial x} + \dfrac{T_y}{R} = 0 \\ \dfrac{\partial T_x}{\partial x} + \dfrac{\partial T_y}{\partial y} - \dfrac{N_y}{R}_{z} = 0 \\ \dfrac{\partial M_x}{\partial x} + \dfrac{\partial M_{yx}}{\partial y} - T_x + \dfrac{PR}{4}\left(\dfrac{\partial U}{\partial z} - \dfrac{\partial W}{\partial x}\right) = 0 \\ \dfrac{\partial M_y}{\partial y} + \dfrac{\partial M_{xy}}{\partial x} - T_y + \dfrac{PR}{2}\left(\dfrac{\partial V}{\partial z} - \dfrac{1}{1+z/R}\left(\dfrac{\partial W}{\partial y} - \dfrac{V}{R}\right)\right) = 0 \end{cases} \tag{6}$$

where P is the hydrostatic external pressure. Finally, after substituting Eqs. (1) to (5) in these governing relations (6), the eigen-value buckling problem can be expressed as:

$$\left([K] + P[L]\right)\begin{Bmatrix} a_u \\ a_v \\ a_w \\ a_{\varphi x} \\ a_{\varphi y} \end{Bmatrix} = \begin{Bmatrix} 0 \\ 0 \\ 0 \\ 0 \\ 0 \end{Bmatrix} \tag{7}$$

where $[K]$ and $[L]$ are 5×5 square matrices. The corresponding K_{ij} and L_{ij} terms are

detailed in Appendix A. The stability limit P_{cr} corresponds to the lowest value of P satisfying Eq. (7).

2.2.2. Genetic algorithm

As mentioned earlier, the optimization problem investigated is a discrete one and then requires adequate procedures dealing with discontinuous design space. Moreover, previous studies dealing with the optimal laminations of composite cylinders subjected to various load cases (axial compression, torsion, lateral pressure) have demonstrated that such problems imply many local optima and non-convexity of the design space [8,9]. The usefulness and efficiency of genetic algorithms for the study of this kind of discrete multi-modal engineering design problems have been explored intensively in recent years [7,13,15,16]. The principle of this robust method can be expressed by applying an analogy with natural evolution: it manipulates a fixed number (called population) of potential design solutions (called individuals). The starting population is randomly created. According to evolutionary theories, only the fittest (i.e. leading to the highest objective function values) individuals are likely to survive and to form a new population. New individuals are obtained by recombining their features using a set of biologically inspired operators (selection, crossover and mutation) [15,16]. This process is renewed for a fixed number of generations and finally yields the best individual found. In this application, each individual manipulated by the created genetic algorithm represents a stacking sequence. Considering Ref. [15] recommendations concerning the efficiency of operators, the tournament selection, the whole arithmetical crossover and the random uniform mutation have been applied. The details of these operators can be found in Refs. [13,15]. Moreover, preliminary tests of performances detailed in Ref. [13] have demonstrated the efficiency of the genetic algorithm procedure developed.

2.3. Results

The numerical examples concern IFREMER's investigations carried out in connection with the composite manufacturer CNIM (Constructions Navales Industrielles de la Méditérannée - Hyères, France). The structures considered are small-scale cylinders of 400 mm length and 175 mm internal diameter. The first constitutive material considered is a carbon fiber reinforced epoxy resin (T700 fibers, F100 resin). According to previous experimental and numerical studies [14], the following orthotropic mechanical properties have been taken (modulus in GPa): $E_1 = 156$; $E_2 = 9.65$; $E_3 = 6.57$; $G_{12} = 5.47$; $G_{13} = 2.8$; $G_{23} = 3.92$; $\nu_{12} = 0.27$; $\nu_{13} = 0.34$; $\nu_{23} = 0.492$. Each cross-ply is assumed to be 0.625 mm thick [13]. Four different thin-walled cylinders have been investigated. Tab. 1 details the corresponding numbers N of cross-plies (from 10 to 19) and the h thickness values. Following the manufacturer's requirements, the cross-ply angles θ_i are limited to five Θ_j available values (in degrees):

$$\theta_i \in \{30\,;45\,;60\,;75\,;90\}$$

The best laminations $[\theta_1/\theta_2/.../\theta_N]_{OPTI}$ obtained using the developed optimization code are given in Tab. 2. The execution of the optimization code did not exceed 45 minutes on a SUN Ultrasparc workstation. For each cylinder studied, it appears that the optimization procedure always lead to typical characteristic $[90_{N1}/\Psi_1/\Phi_{N2}/\Psi_2/90_{N3}]$ laminations, where Ψ_1 and Ψ_2 indicate eventual transition zones (with ply angle values between 45° and 75°) and Φ is the minimum winding angle value (equal to 30°). The corresponding buckling pressures (denoted by $P_{cr}([\theta_1/\theta_2/.../\theta_N]_{OPTI})$, see Tab. 2) have been estimated

by non-linear stability analyses using SAMCEF FEM code: the cylinders were modeled with Mindlin composite laminated shell elements connected to rigid end-closures [13,14]. The critical pressures $P_{cr}([55_N])$ of the $\lfloor 55_N \rfloor$ laminated reference cylinders have also been calculated using this FEM model. It can be stated that the buckling mode is always 'type 2' or 'type 3' (see Fig. 2). The increases of buckling pressures are evaluated using the relative gain factor γ defined as follows:

$$\gamma = \frac{P_{cr}([\theta_1 / \theta_2 / ... / \theta_N]) - P_{cr}([55_N])}{P_{cr}([55_N])}$$

The results detailed in Tab. 2 show that the $[90_{N1}/\Psi_1/30_{N2}/\Psi_2/90_{N3}]$ optimized lamination patterns always induce substantial buckling pressure increase with respect to the orthotropic $\lfloor 55_N \rfloor$ reference solutions: the γ gain values, highest for the thinner cylinders, are always greater than 35%.

The cylinder static strengths has also been checked. For the carbon/epoxy composite material considered, the tension and compression normal stress limits and the shear stress limits are assumed to be (in MPa) [13]: $S_{11}^T = 2220$; $S_{22}^T = 33$; $S_{33}^T = 17$; $S_{11}^C = -1270$; $S_{22}^C = -133$; $S_{33}^C = -124$; $S_{44} = 35$; $S_{55} = 35$; $S_{66} = 70$. For each cylinder, the following safety factor *S* has been calculated:

$$S = P_L / P_{cr}$$

where P_L is the hydrostatic external pressure value leading to the first ply failure calculated by static SAMCEF FEM analysis using the Tsai-Wu criterion and P_{cr} is the critical pressure previously calculated by FEM analysis (see Tab. 2) [6,13]. The *S* values, detailed in Tab. 3, confirm first that the buckling failure risk is predominant for such small cylinders of this

geometry as mentioned by previous studies [4,13]: the P_L values are always more than 2.5 times higher than the corresponding buckling pressures. Moreover, the optimized laminations do not affect noticeably the safety factor: the $S([\theta_1/\theta_2/.../\theta_N]_{OPTI})$ values are always close to those of the reference cylinder $S([55_N])$.

The influence of the reinforcement type has been also examined: additional optimization calculations have been performed for similar cylinders of a glass fiber reinforced epoxy resin (Vetrotex E glass fibers, My 750 epoxy resin) having the following mechanical properties (modulus in GPa) [17]: $E_1 = 45.6$; $E_2 = 16.2$; $E_3 = 16.2$; $G_{12} = 5.83$; $G_{13} = 5.83$; $G_{23} = 5.78$; $\nu_{12} = 0.278$; $\nu_{13} = 0.278$; $\nu_{23} = 0.4$. The optimized stacking sequences $[\theta_1/\theta_2/.../\theta_N]_{OPTI}$ obtained using the optimization code are detailed in Tab. 4. The limits of stability $P_{cr}([\theta_1/\theta_2/.../\theta_N]_{OPTI})$ and $P_{cr}([55_N])$ have been evaluated using the linear buckling FEM model in order to reduce the CPU time. The gain values γ are also included in Tab. 4. It is interesting to note that the optimization procedure always lead to similar $[90_{N1}/\Psi_1/30_{N2}/\Psi_2/90_{N3}]$ optimized lamination patterns, similarly to the previous carbon/epoxy cylinders. The γ gains are lower than for the carbon/epoxy structures (see Tab. 2) but the optimized stacking sequences induced critical pressure increases always exceeding 20%.

As detailed in Ref. [13], the study of the classical laminate stiffness coefficients of membrane, coupling and bending (see Appendix A) shows that such $[90_{N1}/\Psi_1/30_{N2}/\Psi_2/90_{N3}]$ optimized laminations increase the bending stiffness of the cylinders in the (*y*,*z*) plane significantly (see Fig. 3) with respect to the $[55_N]$ solutions. Thus, it could be said that the optimized stacking sequences act as circumferential stiffeners for the composite vessels so inducing an increase of critical buckling pressure.

3. Experiment on a carbon/epoxy cylinder

In order to complete the numerical study of filament wound carbon/epoxy cylinders detailed previously in section §2.3, a first experiment has been carried out. The tube studied is the thinner one having the $[90_2 / 60 / 30_5 / 60 / 90]$ optimized stacking sequence (see Tab. 2). The P_{cr} buckling pressure evaluated by non-linear FEM analysis is 22.5 MPa (see Tab. 2) and the corresponding calculated buckling mode is 'type 3'.

This optimized cylinder has been manufactured by CNIM. An ultrasonic preliminary control performed by IFREMER's laboratories has shown the absence of delamination. The pressure test was performed by DERA (Defense Evaluation and Research Agency, now called QINETIQ, partner in the MAST project) in their hyperbaric testing chamber in Rosyth (UK). Similarly to preceding tests, the hydrostatic pressure loading has been applied following a quasi-static progression. The measured buckling pressure was 21.7 MPa Therefore, the agreement with the numerical prediction is quite close, within 1 MPa which corresponds to a 5% difference. Moreover, axial and circumferential strain gauges placed on the internal cylinder surface have shown that the experimental buckling mode shape was actually of 'type 3'. Thus, although only one thin carbon/epoxy cylinder has been tested, it experimentally confirms the numerical results of section §2.3 and allows a validation of the FEM model.

4. Experiments on glass/epoxy cylinders

The experiments on thin glass/epoxy cylindrical shells have also been carried out in order to compare directly the experimental critical pressures of cylinders having optimized stacking sequences with the P_{cr} values of $[55_N]$ orthotropic reference tubes. Another aim

was to confront the testing results with numerical predictions and to evaluate in this way the accuracy of the FEM model. This study has been performed at the University of Brest in collaboration with the manufacturer STRAGLEN (S^T Laurent en Gâtines, France). The structures considered are cylinders 400 mm long and 152.4 mm internal diameter. The wall-thickness h equal to 4.9 mm is composed of 7 cross-plies. The constitutive material is a glass fiber reinforced epoxy resin (Vetrotex E glass fibers, My 750 epoxy resin). The mechanical properties are those detailed in section §2.3. According to the manufacturer, the winding angles θ_i are only allowed to take six available values (in degrees):

$$\theta_i \in \{15\,;30\,;45\,;60\,;75\,;90\}$$

Applying these parameters, the optimization procedure has determined the best lamination as $[90_3/15_2/90_2]$. Thus, this result appears to be very similar to the previous $[90_{N1}/\Psi_1/\Phi_{N2}/\Psi_2/90_{N3}]$ (Φ being the minimum winding angle) ones detailed in section §2.3. The corresponding buckling pressure and the stability limit of a $[55_7]$ cylinder have been evaluated by applying FEM model of non-linear buckling. The calculated buckling modes are of 'type 3' (see Fig. 2). Considering the P_{cr} values obtained detailed in Tab. 5, the gain factor γ is substantial: the optimized cylinder provides a critical value 40% higher than the $[55_7]$ reference one. Following these numerical results, two cylinders having the $[90_3/15_2/90_2]$ optimized lamination and two $[55_7]$ reference tubes have been manufactured by STRAGLEN.

A specific testing device allowing the control of the instability phenomenon has been developed for this experimental study [18]. As shown in Fig. 5, the composite cylinder is placed in a cylindrical testing hull. The hydrostatic external pressure is generated by the translation of a piston activated by a standard tensile machine. The control of the quasi-

static displacement of the actuator allows the control of the amplitude of the post-buckling displacements and then to maintain cylinders in post-critical configurations [13,18]. The hollow screw-top of the testing hull enables the direct visualization of the buckling mode shapes. The device has been designed to test cylinders attaining nearly 180 mm internal diameters and 800 mm maximum lengths. The limit pressure test is 40 MPa. Previous experimental studies described in Ref. [18] have demonstrated the excellent adaptation of this testing machine for the buckling experiments of thin composite tubes: the instability phenomenon clearly appears on the pressure-piston displacement recording and the buckling mode shapes are easily checked.

The tests on the four manufactured filament-wound cylinders have been carried out using the developed testing device in two sets (each comprising a $[90_3/15_2/90_2]$ and a $[55_7]$ cylinders) assuming similar experimental conditions. For each test, the post-processing provides the external pressure loading evolution as a function of the quasi-static displacement of the piston (see Fig. 5). Fig. 6 presents the evolutions observed for both optimized and reference cylinders of the testing set n°1. Similar behavior was noted for the testing series n°2. The pre-buckling progressions appear to be quasi-linear. At the end, the instability phenomenon clearly emerges. The experimental critical pressure values measured for the two testing groups are detailed in Tab. 5. These results are very consistent: the difference between the two $P_{cr}([90_3/15_2/90_2])$ testing values is less than 4% and becomes zero for the $P_{cr}([55_7])$ results. As generally observed [2,3,9,18], the FEM predictions are higher than the P_{cr} experimental values. Nevertheless, these experimental values corroborate and therewith validate the FEM results: the discrepancies between numerical and experimental stability limits are always below 5%. Also, the tested cylinders have always buckled "via" mode of 'type 3' as stated in FEM simulations. Fig. 7 presents an example of the direct viewing of a tested $[90_3/15_2/90_2]$ cylinder: as can be seen, the three

circumferential half-waves of the buckling mode are clearly detected. This experimental study of glass/epoxy cylinders illustrates perfectly the advantage of optimized stacking sequence design: the gain factor γ is always substantial, the optimized tubes enable about a 40% increase of stability limit with respect to the $[55_7]$ reference solutions.

5. Conclusion

The optimal lamination design of unstiffened thin composite underwater vessels subjected to buckling has been investigated. A numerical optimization tool using a genetic algorithm coupled with an analytical TOSD buckling model has been developed. It enables efficient laminations of tubes subjected to high external pressure to be determined in an acceptable CPU time even for large discrete design space times. The optimized laminations, obtained both for carbon/epoxy and glass/epoxy tubes, are characterized by specific $[90_{N1}/\Psi_1/\Phi_{N2}/\Psi_2/90_{N3}]$ patterns (Ψ_1 and Ψ_2 denoting eventual transition zones and Φ being the minimum winding angle value). The FE analyses have indicated that the optimized laminations induce significant increases, always exceeding several tens of percent, of the buckling pressures with respect to the $[55_N]$ reference cylinder ones.

The buckling test of a carbon/epoxy $[90_2/60/30_5/60/90]$ cylinder has confirmed the improvement the lamination obtained from the optimization procedure and validated the accuracy of the FEM model. The tests on thin glass/epoxy cylinders using a special testing device have also confirmed the interest of the optimized solutions and therefore the robustness of the optimization tool developed: the stability limits of $[90_3/15_2/90_2]$ optimized tubes are 40% higher than those of the $[55_N]$ reference cylinders. The observed buckling pressures, buckling mode shapes and stability increases γ are in good agreement with numerical predictions, therefore validating the FE modeling.

This optimization methodology will be applied soon to the design of half-thick and stiffened composite cylindrical vessels involved in IFREMER's developments. Moreover, current studies performed in IFREMER focus on the evaluation of the initial stress state induced by the filament winding manufacturing process.

6. Acknowledgments

DERA (now called QINETIQ, Rosyth, UK) is gratefully thanked for its test results and contributions. Moreover, the authors wish to acknowledge the "Conseil Régional de Bretagne" and the MAS3-CT97-0091 project "lightweight composite pressure housings for mid-water and benthic applications" of the European Community MAST program which have supported this study.

7. Appendix A

$$K_{11} = A_{11}\,\overline{m}^2 + A_{66}\,\overline{n}^2 \quad ; \quad K_{12} = -\left(A_{12} + A_{66} + \frac{B_{66}}{R} + \frac{4}{3\,R\,h^2}\left(B^a_{12} + B^a_{66}\right)\right)\overline{m}\,\overline{n} \quad ;$$

$$K_{13} = -\frac{A_{12}\,\overline{m}}{R} - \frac{4}{3\,h^2}\left(B^a_{11}\,\overline{m}^3 + \left(B^a_{12} + 2\,B^a_{66}\right)\overline{m}\,\overline{n}^2\right) \quad ;$$

$$K_{14} = B_{11}\,\overline{m}^2 + B_{66}\,\overline{n}^2 - \frac{4}{3\,h^2}\left(B^a_{11}\,\overline{m}^2 + B^a_{66}\,\overline{n}^2\right) \quad ;$$

$$K_{15} = K_{24} = -\left(B_{12} + B_{66} - \frac{4}{3\,h^2}\left(B^a_{12} + B^a_{66}\right)\right)\overline{m}\,\overline{n} \quad ; \quad K_{21} = -\left(A_{12} + A_{66}\right)\overline{m}\,\overline{n} \quad ;$$

$$K_{22} = A_{22}\,\overline{n}^2 + A_{66}\,\overline{m}^2 + \frac{A_{44}}{R^2} - \frac{4\,D_{44}}{R^2\,h^2} + \frac{B_{66}\,\overline{m}^2}{R} + \frac{4}{3\,R\,h^2}\left(B^a_{22}\,\overline{n}^2 + B^a_{66}\,\overline{m}^2\right) \quad ;$$

$$K_{23} = \left(\left(A_{22} + A_{44}\right) - \frac{4\,D_{44}}{h^2}\right)\frac{\overline{n}}{R} + \frac{4}{3\,h^2}\left(B^a_{22}\,\overline{n}^3 + \left(B^a_{12} + 2\,B^a_{66}\right)\overline{m}^2\,\overline{n}\right) \quad ;$$

$$K_{25}=-\frac{A_{44}}{R}+\frac{4\,D_{44}}{R\,h^2}+B_{22}\,\overline{n}^2+B_{66}\,\overline{m}^2-\frac{4}{3\,h^2}\left(B^a_{22}\,\overline{n}^2+B^a_{66}\,\overline{m}^2\right)\ ;$$

$$K_{31}=-\frac{A_{12}\,\overline{m}}{R}\ \ ;\ \ K_{32}=\left(\left(A_{22}+A_{44}\right)-\frac{4\,D_{44}}{h^2}+\frac{4\,B^a_{22}\,\overline{n}}{3\,R\,h^2}\right)\frac{\overline{n}}{R}\ \ ;$$

$$K_{33}=\frac{A_{22}}{R^2}+A_{44}\,\overline{n}^2+A_{55}\,\overline{m}^2-\frac{4}{h^2}\left(D_{44}\,\overline{n}^2+D_{55}\,\overline{m}^2\right)+\frac{4}{3\,R\,h^2}\left(B^a_{12}\,\overline{m}^2+B^a_{22}\,\overline{n}^2\right)\ ;$$

$$K_{34}=\left(A_{55}-\frac{4\,D_{55}}{h^2}-\frac{B_{12}}{R}+\frac{4\,B^a_{12}}{3\,R\,h^2}\right)\overline{m}\ \ ;\ \ K_{35}=\left(-A_{44}+\frac{4\,D_{44}}{h^2}+\frac{B_{22}}{R}-\frac{4\,B^a_{22}}{3\,R\,h^2}\right)\overline{n}\ \ ;$$

$$K_{41}=B_{11}\,\overline{m}^2+B_{66}\,\overline{n}^2\ \ ;\ \ K_{42}=-\left(B_{12}+B_{66}+\frac{D_{66}}{R}+\frac{4}{3\,R\,h^2}\left(D^a_{12}+D^a_{66}\right)\right)\overline{m}\,\overline{n}\ \ ;$$

$$K_{43}=A_{55}\,\overline{m}-\frac{4\,D_{55}\,\overline{m}}{h^2}-\frac{B_{12}\,\overline{m}}{R}-\frac{4}{3\,h^2}\left(D^a_{11}\,\overline{m}^3+\left(D^a_{12}+2D^a_{66}\right)\overline{m}\,\overline{n}^2\right)\ ;$$

$$K_{44}=A_{55}-\frac{4\,D_{55}}{h^2}+D_{11}\,\overline{m}^2+D_{66}\,\overline{n}^2-\frac{4}{3\,h^2}\left(D^a_{11}\,\overline{m}^2+D^a_{66}\,\overline{n}^2\right)\ ;$$

$$K_{45}=K_{54}=\left(-D_{12}-D_{66}+\frac{4}{3\,h^2}\left(D^a_{12}+D^a_{66}\right)\right)\overline{m}\,\overline{n}\ \ ;\ \ K_{51}=-\left(B_{12}+B_{66}\right)\overline{m}\,\overline{n}\ \ ;$$

$$K_{52}=-\frac{A_{44}}{R}+\frac{4\,D_{44}}{R\,h^2}+B_{22}\,\overline{n}^2+B_{66}\,\overline{m}^2+\frac{D_{66}\,\overline{m}^2}{R}+\frac{4}{3\,R\,h^2}\left(D^a_{22}\,\overline{n}^2+D^a_{66}\,\overline{m}^2\right)\ ;$$

$$K_{53}=-A_{44}\,\overline{n}+\frac{4\,D_{44}\,\overline{n}}{h^2}+\frac{B_{22}\,\overline{n}}{R}+\frac{4}{3\,h^2}\left(D^a_{22}\,\overline{n}^3+\left(D^a_{12}+2\,D^a_{66}\right)\overline{m}^2\,\overline{n}\right)\ ;$$

$$K_{55}=A_{44}-\frac{4\,D_{44}}{h^2}+D_{22}\,\overline{n}^2+D_{66}\,\overline{m}^2-\frac{4}{3\,h^2}\left(D^a_{22}\,\overline{n}^2+D^a_{66}\,\overline{m}^2\right)\ ;$$

$$[L]=\begin{bmatrix}0 & 0 & 0 & 0 & 0\\ 0 & 0 & 0 & 0 & 0\\ 0 & 0 & 0 & 0 & 0\\ 0 & 0 & R\,\overline{m}/4 & -R/4 & 0\\ 0 & -1/2 & -\overline{n}/2 & 0 & -R\overline{n}/2\end{bmatrix}$$

Note: the A_{ij}, B_{ij} and D_{ij} lamination terms are the classical laminate stiffness coefficients of membrane, coupling and bending, respectively [6]

$$A_{ij}=\sum_{k=1}^{N}C^{(k)}_{ij}\left(z_k-z_{k-1}\right)\ \ ;\ \ B_{ij}=\frac{1}{2}\sum_{k=1}^{N}C^{(k)}_{ij}\left(z_k^2-z_{k-1}^2\right)\ \ ;\ \ D_{ij}=\frac{1}{3}\sum_{k=1}^{N}C^{(k)}_{ij}\left(z_k^3-z_{k-1}^3\right)$$

The B_{ij}^a and D_{ij}^a terms are additional laminate stiffness coefficients induced by the TOSD displacement field model and defined as follows [13]:

$$B_{ij}^a = \frac{1}{4}\sum_{k=1}^{N} C_{ij}^{(k)}\left(z_k^4 - z_{k-1}^4\right) \quad ; \quad D_{ij}^a = \frac{1}{5}\sum_{k=1}^{N} C_{ij}^{(k)}\left(z_k^5 - z_{k-1}^5\right)$$

8. References

1. Mistry L, Gibson AG & Wu YS. Failure of composite cylinders under combined external pressure and axial loading. Composite Structures 1992;22: p.193-200.
2. Graham D. Composite pressure hulls for deep ocean submersibles. Composite Structures 1995;32: p.331-343.
3. Davies P, Chauchot P. Composites for marine applications – part 2: underwater structures. In: Mechanics of composite materials and structures. Kluwer Academic Pub., 1999. p.249-260
4. Davies P & al. Matériaux composites pour véhicule sous-marin 6000 mètres (Composite materials for a 6000 m underwater vehicle). In: Proceedings of the 10ème Journées Nationales Composites (JNC10), Paris, 29-31 October 1996. p. 525-535.
5. Dvorak GJ, Prochazka P. Thick-walled composite cylinders with optimal fiber prestress. Composites Part B 1996;27b: p.643-649.
6. Gay D. Matériaux composites, 4th edition. Hermès, Paris, 1997.
7. Kogiso N, Watson LT, Gurdal Z & Haftka RT. Genetic algorithm with local improvement for composite laminate design. Structural Optimization 1994;7: p.207-218.
8. Hirano Y. Optimization of laminated composite plate and shells, in: Mechanics of composite materials – recent advances. Pergamon Press 1982. p.355-365.
9. Sun G & Hansen JS. Optimal design of laminated composite circular-cylindrical shells subjected to combined loads. Journal of Applied Mechanics 1988;55: p.136-142.
10. Simitses GJ. Buckling of moderately thick laminated cylindrical shells : a review. Composites Part B 1996;27b: p. 581-587.
11. Soldatos KP. Nonlinear analysis of transverse shear deformable laminated composite cylindrical shells. Journal of Pressure Vessel Technology 1992;114: p. 105-114.

12. Barbe J. Structures coques - équations générales et stabilité. Ensae eds, Toulouse, France, 1983.
13. Messager T. Optimisation d'enceintes sous-marines composites (Optimization of composite submarine hulls). PhD Thesis, Lille University, July 2000.
14. Papazoglou VJ, Tsouvalis NG, Zaphiratou AA. Parametric study of small scale cylinders under hydrostatic load: flat rigid end closures. MAST III project MAS3-CT97-0091, report n° STL-073-F-98. National Technical University of Athens, 1998.

15. Michalewicz Z. Genetic algorithms + data structures = evolution programs, third, revised and extended edition. Springer Verlag Edition, Berlin, 1996.
16. Miettinen K, Neittaanmäki P, Mäkelä MM & Périaux J. Evolutionary Algorithms in Engineering and Computer Science. John Wiley eds, 1999.
17. Soden PD, Hinton MJ, Kaddour AS. Lamina properties, lay-up configurations and loading conditions for a range of fiber reinforced composite laminates. Composite Science and Technology 1998;58(7): p.1011-1022.
18. Gineste B, Grohens A, Messager T. Essais en flambage de tubes composites sous pression externe (Buckling tests of composite tubes subjected to external pressure). Proc. of the 14ème Congrès Français de Mécanique (AUM9), Toulouse, France, 30 August - 3 september 1999.

9. Tables

cylinder number	**1**	**2**	**3**	**4**
number of plies *N*	10	13	16	19
thickness *h* (mm)	6.2	8.1	10.0	11.9

Tab. 1: characteristics of the composite cylinders

cylinder number	$[\theta_1/\theta_2/\ldots/\theta_N]_{OPTI}$	$P_{cr}([\theta_1/\theta_2/\ldots/\theta_N]_{OPTI})$ **(MPa)**	$P_{cr}([55_N])$ **(MPa)**	γ **(%)**
1	$[90_2/60/30_5/60/90]$	22.5	14.2	58.5
2	$[90_2/75/30_8/75/90]$	38.4	26.2	46.6
3	$[90_3/75/45/30_8/60/90_2]$	62.3	44.5	40.0
4	$[90_4/75/60/30_9/90_4]$	90.3	65.1	38.7

Tab. 2: optimized laminations, critical pressures
and stability gains for carbon/epoxy cylinders

cylinder number	**1**	**2**	**3**	**4**
$S([55_N])$	6.9	4.7	3.7	2.9
$S([\theta_1/\theta_2/\ldots/\theta_N]_{OPTI})$	5.3	4.1	3.4	2.5

Tab. 3: safety factor *S* (Tsai-Wu criterion)

cylinder number	$[\theta_1/\theta_2/\ldots/\theta_N]_{OPTI}$	$P_{cr}([\theta_1/\theta_2/\ldots/\theta_N]_{OPTI})$ (MPa)	$P_{cr}([55_N])$ (MPa)	γ (%)
1	$[90_4/30_2/45/90_3]$	11.0	8.5	29.4
2	$[90_3/60/30_7/45/90]$	19.4	15.5	25.2
3	$[90_4/45/30_9/90_2]$	33.9	28.0	21.1
4	$[90_5/60/30_{10}/90_3]$	52.5	43.2	20.8

Tab. 4: optimized laminations, critical pressures
and stability gains for glass/epoxy cylinders

	$P_{cr}([90_3/15_2/90_2])$ (10^5 Pa)	$P_{cr}([55_7])$ (10^5 Pa)	γ (%)
FEM analysis	86.9	61.9	40.4
Testing set n°1	85.8	59.6	44.0
Testing set n°2	82.7	59.7	38.5

Tab. 5: numerical and experimental critical pressures and gains

10. Figures

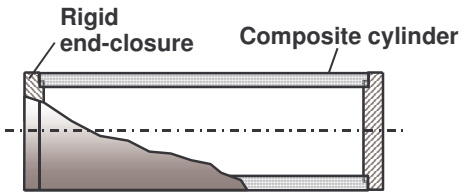

Fig. 1: composite vessel

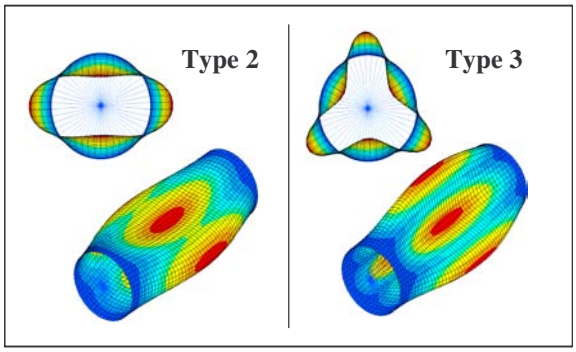

Fig. 2: characteristic buckling modes
of laminated cylinders

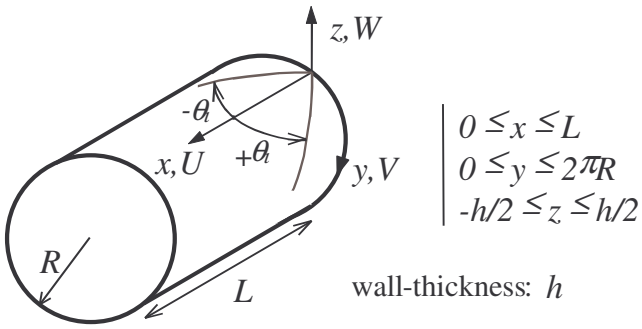

Fig. 3: geometry, coordinates and displacements of cylindrical shell

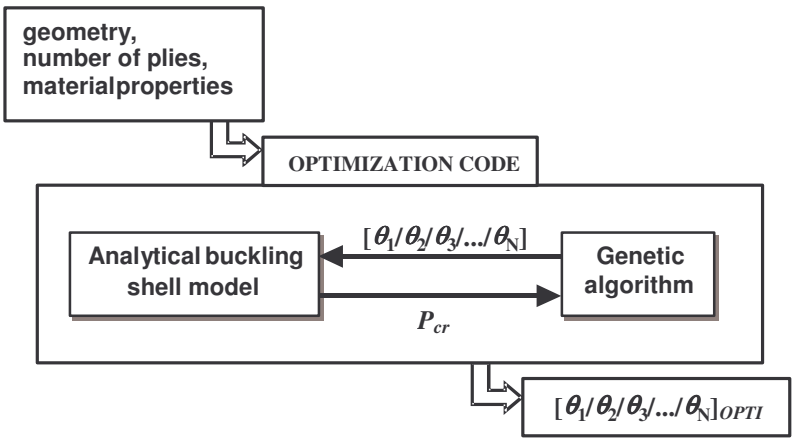

Fig. 4: optimization design tool scheme

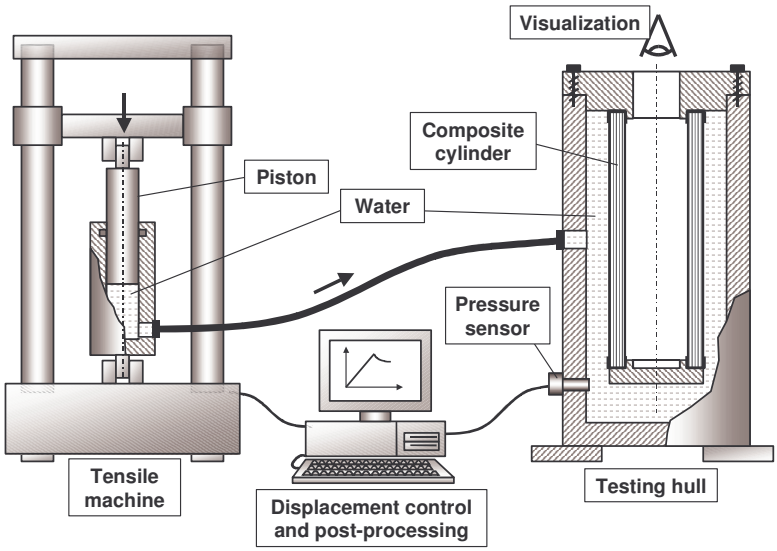

Fig. 5: testing device principle

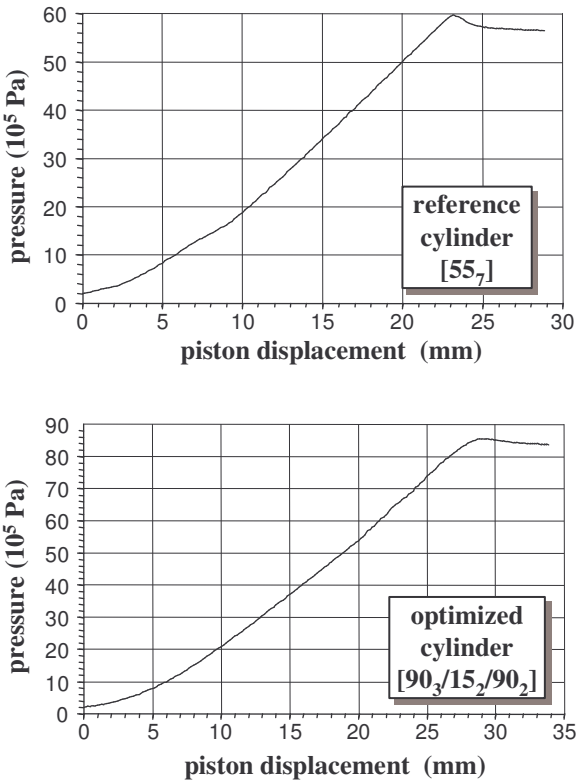

Fig. 6: pressure evolutions of optimized and reference cylinders

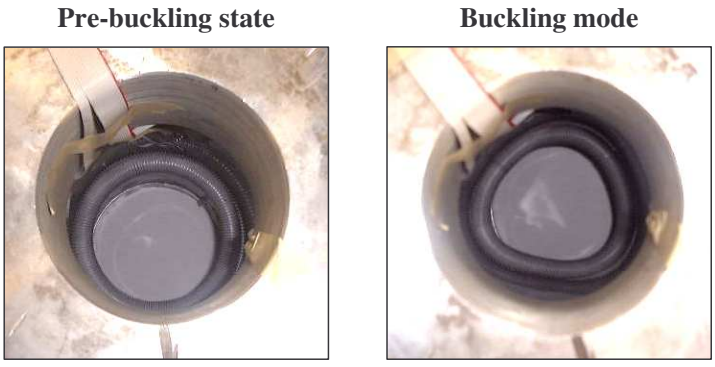

Fig. 7: view of the buckling mode